Available online at www.sciencedirect.com
ScienceDirect
Bioorganic & Medicinal Chemistry 15 (2007) 324–332
Bioorganic & Medicinal Chemistry

Fujita-Ban QSAR analysis and CoMFA study of quinoline antagonists of immunostimulatory CpG-oligodeoxynucleotides

Ekaterina Paliakov,[a] Maged Henary,[a] Martial Say,[a] Steven E. Patterson,[b] Alesia Parker,[a] Lori Manzel,[c] Donald E. Macfarlane,[c] Andrzej J. Bojarski[d] and Lucjan Strekowski[a,*]

[a]*Department of Chemistry, Georgia State University, Atlanta, GA 30302, USA*
[b]*UMN Center for Drug Design, 516 Delaware Street, SE, Minneapolis, MN 55455, USA*
[c]*Veterans Affairs Medical Center and University of Iowa, Iowa City, IA 52242, USA*
[d]*Institute of Pharmacology, Polish Academy of Sciences, 30343 Krakow, Poland*

Received 7 July 2006; revised 18 September 2006; accepted 26 September 2006
Available online 29 September 2006

Abstract—One hundred seven 2-arylquinolin-4-amines were assayed in vitro for inhibition of the immunostimulatory effect of oligodeoxynucleotides containing a CpG-motif. The compounds are functionalized with various basic and non-basic groups at the aryl moiety and at the amino substituent of the quinolin-4-amine, and some of them contain an additional substituent at position 6 or 7 of the quinoline. Activities of these antagonists, expressed as EC_{50} values, range from 0.2 to 200 nM. A statistically significant structure-activity correlation was obtained for the Fujita-Ban variant of the classical Free-Wilson analysis. The CoMFA results derived from several models consistently indicate that electrostatic interactions of the molecules with a biological receptor contribute to biological activities to a greater extent than steric effects.

1. Introduction

Bacterial DNA, oligodeoxynucleotides (ODN), and phosphorothioate ODN are immunostimulatory.[1] The recognition of the foreign DNA by the innate and adaptive immune systems of vertebrates is based upon the extent of methylation of CpG dinucleotide motifs.[2] While in vertebrate DNA about 70% of the cytosines are methylated, bacterial DNA contains mostly unmethylated CpG motifs. The responsiveness of the immune system to CpG-DNA is correlated with expression of the Toll-Like-Receptor-9 (TLR-9)[3] which activates a signal transduction pathway leading to inflammatory responses and the induction of various genes involved in defense system.[4] Macfarlane showed that quinacrine, chloroquine, and analogs inhibit the immunostimulatory effect of CpG-ODN in vitro.[5] Interestingly, quinacrine, chloroquine, and hydroxychloroquine (plaquenil) induce remission of systemic lupus erythematosus and rheumatoid arthritis.[6,7] Oligodeoxynucleotides are actively transported by cells to acidified vesicles. The inhibitory compounds also partition into acidified vesicles, but they have negligible influence on vesicular pH at concentrations required to suppress signal transduction.[8] Recombinant TLR-9 directly binds CpG-ODN at acid pH, and this binding is inhibited by chloroquine and quinacrine.[9] Following these reports we have undertaken a major project aiming at the identification of highly potent antagonists of immunostimulatory bacterial DNA.[8,10–12] Since CpG-ODN mimic the action of bacterial DNA in vitro, this finding has been the basis for the development by Macfarlane of a simple and highly reliable assay in vitro for the effectiveness of potential antagonists.[5] In our previous studies, different classes of compounds have been screened by using this assay and subjected to SAR analyses. It has been shown that the most active compounds are basic quinolin-4-amines substituted at position 2 with an aryl group and the number of basic groups does not correlate with activity. The structure of the biological receptor of the quinoline

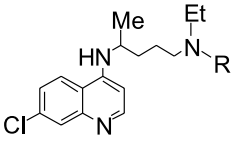

R = Et: chloroquine
R = CH_2CH_2OH: plaquenil

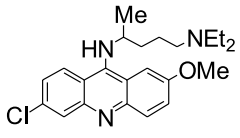

quinacrine

Keywords: Quinolines; CpG; QSAR; CoMFA; TLR-9.
* Corresponding author. Tel.: +1 404 651 0999; fax: +1 404 651 1416; e-mail: Lucjan@gsu.edu

0968-0896/$ - see front matter © 2006 Elsevier Ltd. All rights reserved.
doi:10.1016/j.bmc.2006.09.059

antagonists of immunostimulatory CpG-DNA is not known.

This report describes the Fujita-Ban QSAR analysis and CoMFA study of 107 quinoline antagonists. The results provide guidelines for the design of improved antagonists.

2. Results and discussion

2.1. Quinolines 1–107

The synthesis has been reported elsewhere.[10–23] The general structure together with the structures of various substituents R^1–R^{44} at the quinoline system is given in Table 1. All individual quinolines with the particular substituents R^1–R^{44} are listed in Table 2. The quinolines are substituted at position 2 with 20 aryl groups (R^1–R^{20}), at position 4 with 20 complex amino moieties (R^{21}–R^{40}), and several compounds contain additional substituents (R^{41}–R^{44}) at position 6 or 7.

2.2. Antagonism of immunostimulatory CpG-ODN

The ability of quinoline derivatives to inhibit the action of CpG-ODN was assessed in vitro using WEHI 231 B-cell lymphoma cells as previously described.[5] The experimental activities of individual compounds were expressed as logarithms of the effective molar concentrations at 50% inhibition [$-\log(EC_{50})$]. These values are presented in Table 2 in descending order for a direct, qualitative SAR analysis. The quantitative analyses by using classical QSAR and CoMFA studies are discussed below.

2.3. Classical QSAR

2.3.1. General. The Fujita-Ban QSAR analysis,[24,25] which is a modified Free-Wilson methodology, was conducted with the training set of 101 compounds and the test set of 6 compounds. Compounds of the test set are printed in boldface in Table 2. The individual substituent, from R^1 to R^{44}, at the quinoline is present in at least two molecules, which is the general requirement of this non-parametric analysis. For every compound of the series the experimental values of biological activity (EC_{50}, molar concentrations) used in the logarithmic scale are expressed as the sum of the activity contributions α of the substituents R^1–R^{44}, referring to theoretical biological activity of the arbitrarily chosen reference compound **40**. By definition, the contributions of the substituents R^8 and R^{29} in **40** are taken as zero. A statistically significant function was obtained for the training set of 101 compounds (Eq. 1), where N is number of compounds, r^2 is squared correlation coefficient, s is standard deviation of the regression, and F is value of the Fisher's test.

$$-\log(EC_{50}) = 7.79 + \Sigma\alpha_R$$
$$N = 101, \quad r^2 = 0.886, \quad s = 0.368, \quad F = 10.763 \qquad (1)$$

The corresponding individual contributions α_R of the substituents R are listed in descending order in Table 1. The validity of this model was confirmed by using a randomly selected set of 6 compounds for external predictivity. The results are also summarized in Table 2, showing excellent predictivity. The r^2 value for predictivity is 0.918. The function 1 demonstrates that the partial contributions α_R of substituents at the quinoline to the overall biological activity of the compounds are additive. The physical meaning is that these compounds interact in a specific fashion with the biological receptor, presumably TLR-9. The effects of the particular substituents are summarized as follows.

2.3.2. Aryl group at position 2 of the quinoline. The reference aryl moiety is *para*-tolyl R^8. The *para*-piperazinophenyl R^1 shows the greatest α_R value within the analyzed set of substituents R^1–R^{20}. Inspection of the contributions of isomeric substituted phenyl groups reveals that the α_R values decrease in the order of *para* > *meta* > *ortho*: R^8 (*p*) > R^{11} (*m*) > R^{20} (*o*), R^1 (*p*) > R^7 (*o*), R^3 (*p*) > R^5 (*m*), R^{10} (*p*) > R^{15} (*m*) > R^{17} (*o*), and R^{12} (*m*,*p*) > R^{14} (*o*,*p*). Since these sets of isomeric substituted phenyl groups include both electron-rich and electron-deficient moieties, it can be concluded that the electron density at the aryl group is not a primary determinant of biological activity. Within a series of isomeric molecules the highest activity is observed for molecules without a steric bulk at the *ortho* or *meta* position of the phenyl group. An interesting observation is a relatively high contribution of the *ortho*-[[2-(dimethylamino)ethyl]amino]phenyl group R^4 (Table 1). Accordingly, it can be predicted that the activities of quinolines substituted with the isomeric *para*- or *meta*-($Me_2NCH_2CH_2NH$)Ph group will be greater than those for the corresponding compounds bearing the R^4 (*o*) group.

2.3.3. Substituted amino group at position 4 of the quinoline. The reference amino moiety is [2-(dimethylamino)ethyl]amino (R^{29}). Its analogs show a wide range of α_R values suggesting a highly specific interaction of the substituted molecules with the biological receptor. Interestingly, the non-basic 4-hydroxyphenylamino group R^{40} and its basic 3,5-bis(4-methylpiperazinomethyl)-substituted analog R^{21} show the lowest and the highest contributions, respectively.

2.3.4. Substituents at position 6 or 7 of the quinoline. While the chlorine (R^{41}) and fluorine (R^{42}) atoms at position 6 and the trifluoromethyl group (R^{44}) at position 7 of the quinoline are electron-withdrawing, the phenyl group (R^{43}) is electron-donating relative to the electron-deficient quinoline system. All R^{41}–R^{44}-substituted quinolines show decreased activity relative to their unsubstituted counterparts, suggesting unfavorable steric interactions of the substituted molecules with the receptor.

2.4. CoMFA

2.4.1. Conformational analysis. Comparative molecular field analysis is used to calculate electrostatic and steric properties of the molecules according to the respective Coulomb and Lennard-Jones potentials.[26] The generated models characterize relative changes in magnitude of

Table 1. Substituents R at positions 2, 4, 6, and 7 of the quinoline in compounds **1**–**107** and substituent contributions α_R from Fujita-Ban analysis

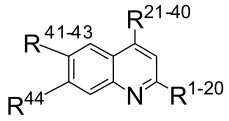

1-107

R	α_R	R	α_R	R	α_R
R^1 = 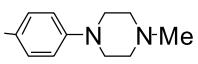	1.092	R^{14} = 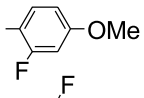	-0.480	R^{28} = 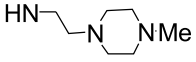	0.015
R^2 = 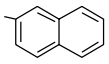	0.757	R^{15} = 	-0.664	R^{29} = 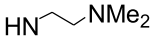	0.000
R^3 = 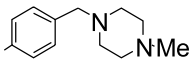	0.433	R^{16} = 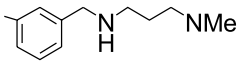	-0.761	R^{30} = 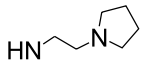	-0.005
R^4 = 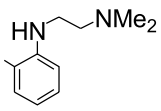	0.407	R^{17} = 	-0.970	R^{31} = 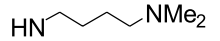	-0.013
				R^{32} = 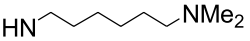	-0.082
		R^{18} = 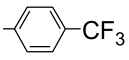	-1.010	R^{33} = 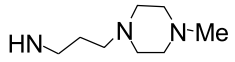	-0.180
R^5 = 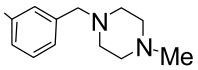	0.217	R^{19} = 	-1.140	R^{34} = 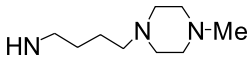	-0.205
R^6 = 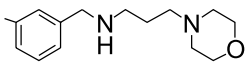	0.155	R^{20} = 	-1.262	R^{35} = 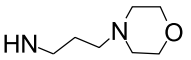	-0.238
R^7 = 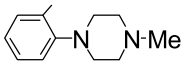	0.038	R^{21} = 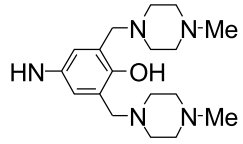	1.142	R^{36} = 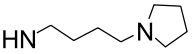	-0.290
R^8 = 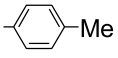	0.000	R^{22} = 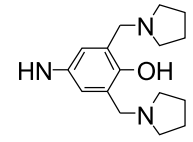	0.766	R^{37} = 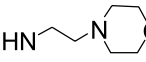	-0.790
R^9 = 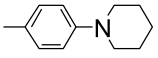	-0.020	R^{23} = 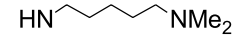	0.173	R^{38} = 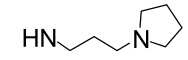	-0.874
R^{10} = 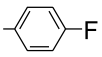	-0.155	R^{24} = 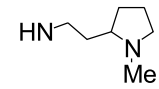	0.158	R^{39} = 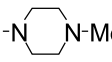	-0.954
R^{11} = 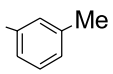	-0.247	R^{25} = 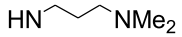	0.098	R^{40} = 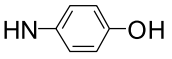	-1.419
R^{12} = 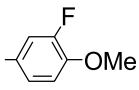	-0.335	R^{26} = 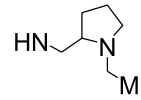	0.039	R^{41} = Cl	-0.182
R^{13} = 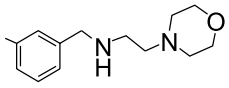	-0.423	R^{27} =	0.022	R^{42} = F	-0.363
				R^{43} = Ph	-0.730
				R^{44} = CF_3	-1.082

electrostatic and steric fields as a function of the sample chosen from the data set. Geometry of molecules must be optimized in the first step.[26] One of the major features of 2-arylquinolines is equilibrium conformation around the torsional bond of the quinoline-aryl system. In this work, the geometry in solution of a template molecule **2** was studied by proton NOE NMR, and then the results were compared with the computed structures of **2** using two force fields, namely MMFF94 field and Tripos field, as implemented in the SYBYL program. Since

Table 2. Experimental and predicted activities of the training set of 101 quinolines and the test set[a] of 6 quinolines using Fujita-Ban QSAR analysis and CoMFA study

Quinoline	Substituent at				Activity, $-\log(EC_{50})$[b]				
						Calculated			
	C2	C4	C6	C7	Exptl[a]	CoMFA	Residual	Fujita-Ban	Residual
1	R^2	R^{21}	—	—	9.62	9.52	0.10	9.51	0.11
2	R^1	R^{29}	—	—	9.12	8.97	0.15	8.88	0.24
3	R^1	R^{25}	—	—	9.00	8.60	0.40	8.98	0.02
4	R^2	R^{22}	—	—	8.94	8.98	−0.04	9.13	−0.19
5	R^1	R^{31}	—	—	8.91	8.91	0.00	8.87	0.04
6[a]	R^1	R^{23}	—	—	8.84	8.76	0.08	9.06	−0.22
7	R^8	R^{21}	—	—	8.84	8.72	0.12	8.93	−0.09
8	R^1	R^{29}	R^{41}	—	8.84	8.68	0.16	8.70	0.14
9	R^1	R^{28}	—	—	8.82	8.76	0.06	8.90	−0.08
10	R^{10}	R^{21}	—	—	8.76	8.66	0.10	8.78	−0.02
11	R^8	R^{22}	—	—	8.75	8.86	−0.11	8.56	0.19
12	R^1	R^{32}	—	—	8.72	8.77	−0.05	8.80	−0.08
13	R^1	R^{24}	—	—	8.70	8.75	−0.05	9.04	−0.34
14	R^2	R^{24}	—	—	8.69	8.62	0.07	8.52	0.17
15[a]	R^1	R^{35}	—	—	8.66	8.58	0.08	8.65	0.02
16	R^1	R^{30}	—	—	8.62	8.83	−0.21	8.88	−0.26
17	R^1	R^{39}	—	—	8.57	8.39	0.18	7.93	0.64
18	R^3	R^{30}	—	—	8.49	8.21	0.28	8.22	0.27
19	R^1	R^{37}	—	—	8.48	8.30	0.18	8.09	0.39
20	R^2	R^{35}	—	—	8.45	8.32	0.13	8.13	0.32
22	R^2	R^{31}	—	—	8.40	8.38	0.02	8.35	0.05
21	R^5	R^{25}	—	—	8.43	8.32	0.11	8.11	0.32
23	R^1	R^{34}	—	—	8.31	8.31	0.00	8.68	−0.37
24	R^9	R^{29}	—	—	8.27	8.31	−0.04	7.77	0.49
25[a]	R^2	R^{26}	—	—	8.27	7.64	0.63	8.41	−0.14
26	R^{10}	R^{31}	—	—	8.26	8.53	−0.27	8.30	−0.04
27	R^1	R^{36}	—	—	8.26	8.66	−0.40	8.59	−0.33
28	R^4	R^{31}	—	—	8.23	8.20	0.03	8.18	0.05
29	R^2	R^{32}	—	—	8.23	8.51	−0.28	8.28	−0.05
30	R^4	R^{29}	—	—	8.19	7.95	0.24	8.20	−0.01
31	R^2	R^{29}	R^{43}	—	8.19	8.27	−0.08	7.64	0.55
32	R^3	R^{33}	—	—	8.17	8.28	−0.11	8.04	0.13
33	R^3	R^{29}	—	—	8.15	7.88	0.27	8.22	−0.07
34	R^5	R^{24}	—	—	8.11	8.35	−0.24	8.17	−0.06
35	R^3	R^{25}	—	—	8.04	8.31	−0.27	8.32	−0.28
36	R^2	R^{29}	—	—	8.04	8.19	−0.15	8.37	−0.33
37[a]	R^2	R^{25}	—	—	7.96	8.04	−0.08	8.46	−0.50
38	R^8	R^{25}	—	—	7.94	7.71	0.23	7.89	0.05
39	R^6	R^{37}	—	—	7.92	8.12	−0.20	7.16	0.76
40	R^8	R^{29}	—	—	7.91	7.62	0.29	7.89	0.02
41	R^{10}	R^{24}	—	—	7.88	8.08	−0.20	7.79	0.09
42	R^{11}	R^{25}	—	—	7.88	7.71	0.17	7.64	0.24
43	R^7	R^{29}	R^{42}	—	7.88	7.84	0.04	7.47	0.41
44	R^2	R^{38}	—	—	7.87	7.65	0.22	7.49	0.38
45	R^{11}	R^{31}	—	—	7.86	7.68	0.18	7.73	0.13
46	R^8	R^{33}	—	—	7.86	7.95	−0.09	7.61	0.25
47	R^{11}	R^{24}	—	—	7.85	7.93	−0.08	7.70	0.15
48	R^{10}	R^{23}	—	—	7.81	7.62	0.19	7.81	0.00
49	R^9	R^{25}	—	—	7.80	8.17	−0.37	7.87	−0.07
50	R^{10}	R^{34}	—	—	7.80	7.78	0.02	7.43	0.37
51	R^{10}	R^{26}	—	—	7.77	7.68	0.09	7.68	0.09
52	R^{10}	R^{31}	—	—	7.76	7.50	0.26	7.62	0.14
53	R^{11}	R^{29}	—	—	7.74	7.48	0.26	7.54	0.20
54	R^{10}	R^{28}	—	—	7.73	7.56	0.17	7.65	0.08
55	R^8	R^{27}	—	—	7.73	7.57	0.16	7.81	−0.08
56	R^{13}	R^{25}	—	—	7.69	7.71	−0.02	7.47	0.22
57	R^{10}	R^{32}	—	—	7.69	7.64	0.05	7.55	0.14
58	R^{10}	R^{36}	—	—	7.68	7.40	0.28	7.35	0.33
59	R^{11}	R^{26}	—	—	7.66	7.71	−0.05	7.58	0.08
60	R^8	R^{26}	—	—	7.66	7.89	−0.23	7.83	−0.17
61	R^{11}	R^{27}	—	—	7.65	7.73	−0.08	7.57	0.08
62	R^{10}	R^{30}	—	—	7.62	7.40	0.22	7.63	−0.01

(*continued on next page*)

Table 2 (*continued*)

Quinoline	Substituent at				Activity, $-\log(EC_{50})$[b]				
						Calculated			
	C2	C4	C6	C7	Exptl[a]	CoMFA	Residual	Fujita-Ban	Residual
63	R^8	R^{35}	—	—	7.57	7.60	−0.03	7.55	0.02
64	R^{11}	R^{33}	—	—	7.56	7.51	0.05	7.36	0.20
65	R^{12}	R^{29}	—	—	7.45	7.43	0.02	7.46	−0.01
66	R^7	R^{29}	—	—	7.41	7.54	−0.13	7.83	−0.42
67	R^{14}	R^{29}	—	—	7.38	7.18	0.20	7.31	0.07
68	R^9	R^{31}	—	—	7.33	7.67	−0.34	7.76	−0.43
69	R^{11}	R^{35}	—	—	7.30	7.37	−0.07	7.31	−0.01
70	R^{10}	R^{29}	—	—	7.29	7.41	−0.12	7.64	−0.35
71	R^6	R^{25}	—	—	7.28	7.35	−0.07	8.04	−0.76
72[a]	R^{10}	R^{29}	R^{41}	—	7.28	6.82	0.46	7.45	−0.17
73	R^3	R^{39}	—	—	7.23	7.22	0.01	7.27	−0.04
74	R^{10}	R^{35}	—	—	7.17	7.38	−0.21	7.40	−0.23
75	R^{11}	R^{29}	—	—	7.14	7.17	−0.03	7.54	−0.40
76	R^{12}	R^{29}	R^{42}	—	7.10	6.85	0.25	7.09	0.01
77	R^5	R^{39}	—	—	7.00	7.13	−0.13	7.05	−0.05
78	R^8	R^{38}	—	—	6.98	7.04	−0.06	6.92	0.06
79	R^{17}	R^{25}	—	—	6.97	7.16	−0.19	6.92	0.05
80	R^{17}	R^{31}	—	—	6.97	6.75	0.22	6.81	0.16
81	R^5	R^{38}	—	—	6.92	7.04	−0.12	7.13	−0.21
82	R^7	R^{39}	—	—	6.88	7.03	−0.15	6.87	0.01
83	R^{14}	R^{29}	R^{42}	—	6.85	6.85	0.00	6.95	−0.10
84	R^8	R^{40}	—	—	6.82	6.76	0.06	6.37	0.45
85	R^{18}	R^{29}	—	—	6.81	6.95	−0.14	6.78	0.03
86	R^{16}	R^{37}	—	—	6.81	6.58	0.23	6.24	0.57
87	R^{19}	R^{29}	—	—	6.79	6.89	−0.10	6.65	0.14
88	R^{20}	R^{25}	—	—	6.73	6.61	0.12	6.63	0.10
89	R^{10}	R^{38}	—	—	6.72	6.80	−0.08	6.76	−0.04
90	R^{11}	R^{38}	—	—	6.71	6.85	−0.14	6.67	0.04
91	R^{17}	R^{24}	—	—	6.69	6.90	−0.21	6.82	−0.13
92	R^{15}	R^{29}	R^{42}	—	6.55	6.59	−0.04	6.76	−0.21
93	R^2	R^{40}	—	—	6.50	6.61	−0.11	6.95	−0.45
94	R^{18}	R^{29}	R^{42}	—	6.39	6.76	−0.37	6.42	−0.03
95[a]	R^{12}	R^{29}	—	R^{44}	6.39	6.36	0.03	6.37	0.02
96	R^{10}	R^{37}	—	—	6.38	6.24	0.14	6.85	−0.47
97	R^{17}	R^{29}	R^{42}	—	6.38	6.35	0.03	6.46	−0.08
98	R^{19}	R^{29}	R^{41}	—	6.33	6.36	−0.03	6.47	−0.14
99	R^8	R^{37}	—	—	6.31	6.49	−0.18	7.00	−0.69
100	R^{10}	R^{29}	—	R^{44}	6.31	6.35	−0.04	6.55	−0.24
101	R^{16}	R^{33}	—	—	6.28	6.35	−0.07	6.85	−0.57
102	R^{13}	R^{38}	—	—	6.27	6.28	−0.01	6.49	−0.22
103	R^{14}	R^{29}	—	R^{44}	6.26	6.36	−0.10	6.23	0.03
104	R^{15}	R^{29}	—	R^{44}	6.26	6.08	0.18	6.05	0.21
105	R^{11}	R^{37}	—	—	6.19	6.31	−0.12	6.75	−0.56
106	R^{20}	R^{35}	—	—	6.19	6.08	0.11	6.29	−0.10
107	R^2	R^{39}	R^{43}	—	6.13	6.19	−0.06	6.68	−0.55

[a] Compounds of the test set.
[b] EC_{50} is an effective molar concentration for 50% inhibition.

the use of the former force field produced a better approximation of the experimentally derived conformation, this force field was chosen for energy minimizations of all molecules. Specifically, the distance d_1 of 2.30 Å (Fig. 1) between protons quinoline-H3 and phenyl-H2 was obtained from the NOESY spectrum by using the distance d_2 of 2.44 Å between the protons phenyl-H2 and phenyl-H3 as the reference.[27] This experimental distance d_1 corresponds to the torsional angle of 30°, which is in excellent agreement with the values reported previously for similar unfused biaromatic systems.[28] The distance d_1 of 2.35 Å and the torsional angle of 34° were calculated using the MMFF94 field. By contrast, the respective values of 2.53 Å and 47° were obtained with Tripos field. A possible effect of solvation on conformation of **2** was also examined by using the Molecular Silverware option in the SYBYL program. However, the simulated solvation with either force field did not result in a significant conformational change. Accordingly, the subsequent energy minimizations for all molecules were conducted without solvation using MMFF94 field.

An important problem is the preferred orientation (twisted *s-trans* or *s-cis*, A or B in Figure 2) of the *ortho* or *meta* substituted phenyl group at position 2 of the quinoline relative to the N1 atom of the quinoline.

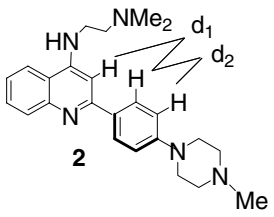

Figure 1. Conformational analysis of quinoline **2** by proton NOE NMR.

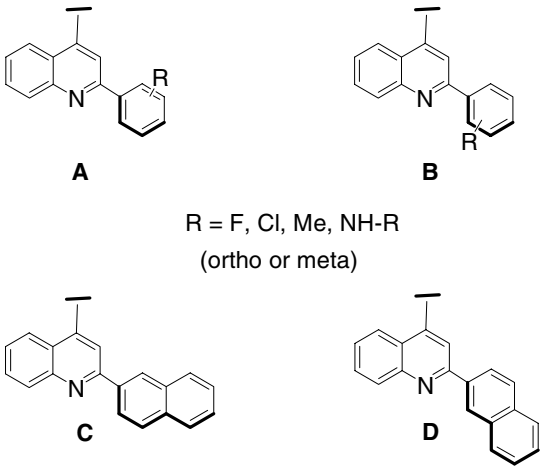

Figure 2. Conformations A–D of 2-substituted quinolines.

For all analyzed compounds of this subgroup the energy minimization results indicated consistently that the energy difference between *s-cis* and *s-trans* structures is less than 1 kcal/mol. Nevertheless, on the basis of the results of our previous qualitative work, it is highly unlikely that *ortho*- and *meta*-phenyl substituted phenylquinolines, especially those with large amino moieties, would interact randomly in two strikingly different conformations (A and B) with a biological receptor.[10–12] Due to the conformational uncertainty, the subsequent development of CoMFA models was conducted separately with both conformations A and B (where applicable). The energy difference is negligible and the torsional angle is identical for the two possible conformations C and D of 2-(2-naphthyl)quinolines. Partial CoMFA models derived from 2-(2-naphthyl)quinolines were identical for C and D conformations. In order to simplify the calculations the complete studies were conducted with conformation C only. All minimized structures were aligned by fitting the quinoline, phenyl-C1, and phenyl-C4 atoms on the template molecule **2**. The results for the two possible orientations A and B are visualized in Figure 3. As can be seen, the alignment A provides a slightly better fit in comparison to the alternative alignment B. While the quinoline systems of all compounds are superimposed with high accuracy, the 2-aryl rings are deviated from co-planarity with the quinoline core in both geometries A and B. Moreover, this deviation from co-planarity, as indicated by the computed torsional angle Quin-C3–QuinC2–Ph-C1–Ph-C2 (optimized for all individual compounds), varies depending on a substituent at the phenyl group. As expected, the largest values of the computed torsional angles are observed for phenylquinolines with an *ortho* substituent at the phenyl group. This feature has important ramifications for the results of the CoMFA study (vide infra).

2.4.2. CoMFA models. Six models were generated by using electrostatic and steric fields (Table 3). The parameter n is defined as an index of the degree of complexity of the model. In this work, the number of principal components n corresponds to the lowest value of a standard error of prediction S_{PRESS}, and the highest value of a cross-validated squared correlation coefficient q^2, as calculated by SAMPLS routine in SYBYL. Two sets, each comprising of three models, I–III and IV–VI, were generated by using molecular alignments A and B. Analyses of the statistical evaluation parameters for all models in Table 3 consistently show that the electrostatic and steric fields of the molecules are both important for

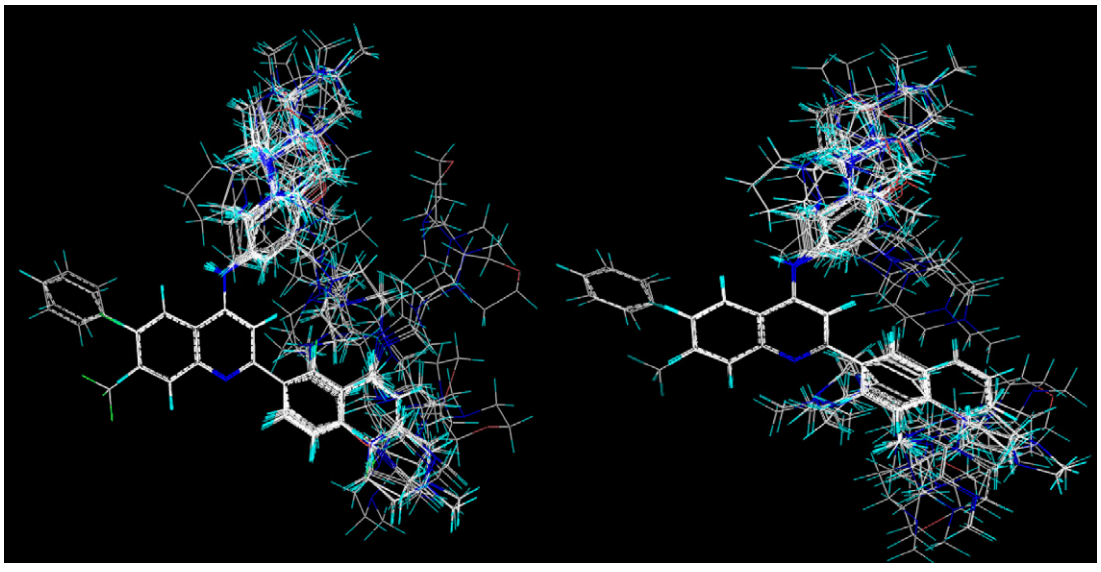

Figure 3. Alignments for orientations A (left) and B (right) of 107 CpG-ODN inhibitors used for CoMFA models given in Table 3.

Table 3. Statistical results of CoMFA PLS analysis[a,b]

CoMFA model	CoMFA field	Alignment based on conformation	q^2	n	S_{PRESS}	r^2	SE	F	Field %
I	$e + s$	A	0.626	6	0.524	0.958	0.176	399.96	e (60) s (40)
II	e	A	0.598	3	0.535	0.829	0.349	355.56	e (100)
III	s	A	0.492	2	0.598	0.670	0.482	243.22	s (100)
IV	$e + s$	B	0.491	4	0.604	0.878	0.269	156.83	e (57) s (43)
V	e	B	0.530	3	0.578	0.820	0.358	99.49	e (100)
VI	s	B	0.478	2	0.606	0.458	0.665	172.56	s (100)

[a] *Abbreviations:* PLS, partial least squares; s, steric; e, electrostatic; q^2, cross-validated squared correlation coefficient; n, number of components (latent variables); S_{PRESS}, standard error of prediction; PRESS, predictive residual sum of squares; r^2, squared correlation coefficient; SE, standard error of prediction; F, value of the Fisher test.

[b] The leave-one-out (LOO) cross-validated q^2 and explanatory r^2 values were obtained with regard to number of components n. The optimal n value was determined by selecting the smallest S_{PRESS} value. See the text for L10O cross-validations.

biological activity. With two fields used for calculations (models I and IV), the computational results show that the contribution of the electrostatic features to activity is greater than that of steric effects. Even the use of electrostatic field alone provided acceptable models II and V. Conversely, the use of steric field alone for the molecular alignments A and B resulted in generation of the respective models III and VI that are statistically much less significant. Overall, comparison of the respective pairs of models (I/IV, II/V, and III/VI) based on the superimpositions A and B points out to a greater significance of the former alignment. Accordingly, it can be suggested that the substituted phenylquinolines interact in conformation A with the biological receptor.

A graph of predicted versus experimental activities for the most significant model I, obtained with the training set of 101 molecules, is given in Figure 4. The robustness of this model was externally validated by using four independent approaches. First, a high value of a correlation coefficient for predictivity ($r^2_{pred} = 0.867$) was calculated using a test set of six compounds (Table 2). Second, bootstrapping was carried out (100 runs), in order to determine a degree of a statistical confidence. The high value of the coefficient ($r^2_{boot} = 0.970$) with a standard deviation SE of 0.019 provides a high level of confidence for the predictivity of model I. Third, a common test for chance correlation is scrambling of data followed by the leave-one-out (LOO) PLS analysis. The procedure was performed 10 times on randomized activity sets, and in all cases the q^2 values close to zero or negative were obtained. Fourth, the leave-10-out (L10O) cross-validation was performed 10 times, where 10 compounds were left out randomly from each calculation but only once. For the 10 runs the respective values of q^2 and S_{PRESS} ranged from 0.557 to 0.679 and from 0.495 to 0.571. These results provide a strong support for validity of the CoMFA model I.

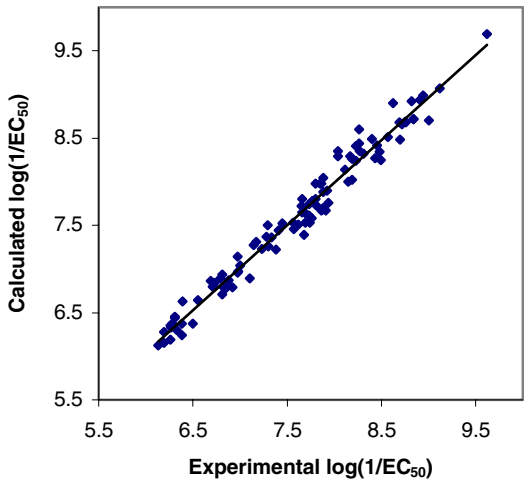

Figure 4. Plot of predicted vs experimental activities for 101 compounds of the training set using CoMFA model I.

An important output from CoMFA is contour maps that show significance of the electrostatic and steric energy values for biological potency. These contours superimposed on one of the bioactive molecules provide a graphic guide to the design of new molecules. The CoMFA contour map for model I on a selected molecule **3** as an example is shown in Figure 5. As can be seen from the electrostatic map on the left, the electrostatic factor is mostly important for the amino side chain at position 4 of the quinoline. It can be suggested that this terminal amino group binds with a weakly acidic group of the biological receptor in a specific manner to form a strong hydrogen-bonding interaction or an ammonium salt. Both phenomena are electrostatic in nature and can be described by the same function on a continuous energy surface. On the other hand, the steric contour map on the right of Figure 5 shows a large yellow area for unfavorable steric contributions. This area extends from the methylene moiety of the 4-methylpiperazino substituent (shown as an example) to the C5-H and C6-H portions of the phenyl group, even though this site of the phenyl group does not bear any substituents in the examined set of compounds. We strongly believe that this outcome reflects the various torsional angles between the quinoline and the phenyl group in compounds with *ortho*, *meta*, and *para* substituents. More specifically, the increase in the torsional angle from para- to meta- (buttressing effect on C2-H) to ortho-substituted derivatives corresponds to rotation of the phenyl group, which is expressed in the steric contour map as an unfavorable steric volume around

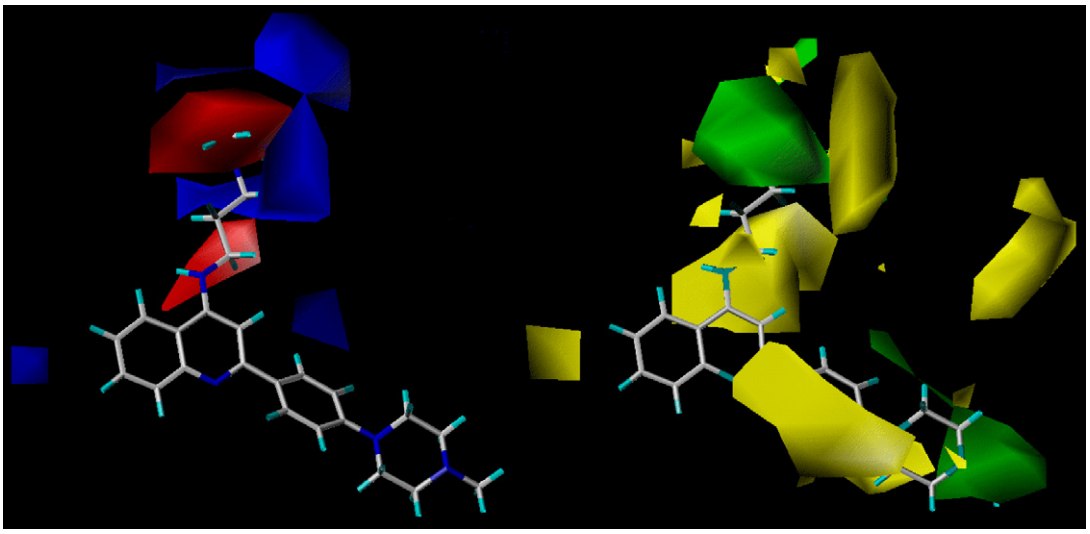

Figure 5. CoMFA contour maps for model I with compound **3** inside the fields. In the electrostatic contour map on the left the red polyhedrals indicate areas where partial negative charge favors activity and the blue polyhedrals display areas where partial negative charge disfavors activity. In the steric contour map on the right the green contours indicate areas where steric bulk increases activity, while yellow contours indicate areas where steric bulk decreases activity.

C5-H and C6-H of the phenyl group. This suggestion is consistent with a relatively low torsional angle of the bioactive conformation of the ligands. An increase in the torsional angle for *meta*- and *ortho*-substituted derivatives would result in a decrease of biological activity, as independently shown by a classical QSAR analysis.

The steric contour map shows that the presence of a bulky substituent at position 6 or 7 at the quinoline decreases activity, also as already suggested by the classical QSAR analysis.

2.5. Conclusions

Classical and 3D QSAR analyses results complement each other and clearly provide guidelines for the design of new antagonists. Within the class of *N*-substituted 2-phenylquinolin-4-amines the most promising candidates are derivatives containing an additional amino side chain at the *para* position of the phenyl group. Both the classical QSAR and CoMFA studies consistently suggest that the aryl group of 2-arylquinolines may interact with a quite narrow pocket on the receptor, primarily by hydrophobic interaction.

3. Methodology

3.1. Biological evaluation

The ability of test compounds to reverse the action of CpG-ODN on WEHI 231 murine lymphoma B-cells was assessed in vitro as described previously.[5,12a]

3.2. Fujita-Ban QSAR

A model was constructed using 44 variables (different substituents at positions 2, 4, 6, and 7 of the quinoline system) and the experimental activities [$-\log(EC_{50})$], molar concentrations] of 101 compounds of the training set. To determine how the substituents contribute to the biological activity, the partial least-squares (PLS) analysis was carried out as implemented in the QSAR/CoMFA on SYBYL program. The model was validated using an independent test set of 6 compounds (Table 2).

3.3. CoMFA

The interatomic distance d_2 for an equilibrium conformation of **2** in solution (Fig. 1) was obtained from a NOESY experiment by using a general procedure.[27] The spectrum was recorded for a solution of **2** in $CDCl_3$ because the low dielectric constant of this solvent is approximated well by the subsequent in vacuo computations of the molecular structures. All molecular modeling calculations were performed with SYBYL 6.9 software running on SGI O_2 workstation. Energy minimizations were performed using MMFF94 force field and the minimum energy change of 0.01 kcal/mol/Å as a convergence criterion. Charges were calculated using the MMFF94 method as implemented in SYBYL. Conformational flexibility of the molecules was taken into account by a systematic conformational search (GRID option, torsion angle C-QuinN^4-QuinC4-QuinC3 with 10° increments). The lowest energy rotamer was further minimized and the minimized structure was used for alignment. The steric and electrostatic field energies were calculated using sp^3 carbon probe atom with +1 charge. Values of the steric and electrostatic energies were truncated at 30 kcal/mol. The CoMFA QSAR equations were calculated with the PLS algorithm, and cross-validation was performed using leave-one-out (LOO) procedure. The models were constructed and validated with the same sets of compounds used in the classical QSAR analysis.

References and notes

1. Krieg, A. M. *Trends Microbiol.* **2001**, *9*, 249, and references cited therein.
2. Ashkar, A. A.; Rosenthal, K. L. *Curr. Mol. Med* **2002**, *2*, 545.
3. Hemmi, H.; Takeuchi, O.; Kawai, T.; Kaisho, T.; Sato, S.; Sanjo, H.; Matsumoto, M.; Hoshino, K.; Wagner, H.; Takeda, K.; Akira, S. *Nature (London)* **2000**, *408*, 740.
4. Beutler, B. *Mol. Immunol.* **2004**, *40*, 845.
5. Macfarlane, D. E.; Manzel, L. *J. Immunol.* **1998**, *160*, 1122.
6. Fox, R. I. *Semin. Arthritis Rheum.* **1993**, *23*, 82.
7. Wallace, D. J. *Rheum. Dis. Clin. North Am.* **1994**, *20*, 243.
8. Manzel, L.; Strekowski, L.; Ismail, F. M. D.; Smith, J. C.; Macfarlane, D. E. *J. Pharmacol. Exp. Therap.* **1999**, *291*, 1337.
9. Rutz, M.; Metzger, J.; Gellert, T.; Luppa, P.; Lipford, G. B.; Wagner, H.; Bauer, S. *Eur. J. Immunol.* **2004**, *34*, 2541.
10. Strekowski, L.; Zegrocka, O.; Henary, M.; Say, M.; Mokrosz, M. J.; Kotecka, B. M.; Manzel, L.; Macfarlane, D. E. *Bioorg. Med. Chem. Lett.* **1999**, *9*, 1819.
11. Strekowski, L.; Say, M.; Zegrocka, O.; Tanious, F. A.; Wilson, W. D.; Manzel, L.; Macfarlane, D. E. *Bioorg. Med. Chem.* **2003**, *11*, 1079.
12. (a) Strekowski, L.; Say, M.; Henary, M.; Ruiz, P.; Manzel, L.; Macfarlane, D. E.; Bojarski, A. J. *J. Med. Chem.* **2003**, *46*, 1242; (b) Henary, M. *Ph. D. Dissertation*, Georgia State University, 2000; (c) Paliakov, E. *Ph. D. Dissertation*, Georgia State University, 2004.
13. Strekowski, L.; Patterson, S. E.; Janda, L.; Wydra, R. L.; Harden, D. B.; Lipowska, M.; Cegla, M. T. *J. Org. Chem.* **1992**, *57*, 196.
14. Strekowski, L.; Mokrosz, J. L.; Honkan, V. A.; Czarny, A.; Cegla, M. T.; Wydra, R. L.; Patterson, S. E.; Schinazi, R. F. *J. Med. Chem.* **1991**, *34*, 1739.
15. Wilson, W. D.; Zhao, M.; Patterson, S. E.; Wydra, R. L.; Janda, L.; Strekowski, L.; Schinazi, R. F. *Med. Chem. Res.* **1992**, *2*, 102.
16. Zhao, M.; Janda, L.; Nguyen, J.; Strekowski, L.; Wilson, W. D. *Biopolymers* **1994**, *34*, 61.
17. (a) Strekowski, L.; Janda, L.; Patterson, S. E.; Nguyen, J. *Tetrahedron* **1996**, *52*, 3273; (b) Say, M. *Ph. D. Dissertation*, Georgia State University, 2001.
18. Paliakov, K.; Henary, M.; Say, M.; Janda, L.; Manzel, L.; Macfarlane, D. E.; Strekowski, L. *Heterocycl. Commun.* **2006** (in press).
19. (a) Strekowski, L.; Parker, A. N.; Hojjat, M.; Say, M.; Zegrocka-Stendel, O.; Patterson, S. E.; Tanious, F. A. *Acta Pol. Pharm., Suppl.* **2004**, *61*, 70; (b) Parker A.N. *Ph. D. Dissertation*, Georgia State University, 1998.
20. Janda, L.; Nguyen, J.; Patterson, S. E.; Strekowski, L. *J. Heterocycl. Chem.* **1992**, *29*, 1753.
21. Strekowski, L.; Zegrocka, O.; Windham, C.; Czarny, A. *Org. Proc. Res. Dev.* **1997**, *1*, 384.
22. Chaires, J. B.; Ren, J.; Henary, M.; Zegrocka, O.; Bishop, G. R.; Strekowski, L. *J. Am. Chem. Soc.* **2003**, *125*, 7272.
23. Say, M.; Paliakov, E.; Henary, M.; Strekowski, L. *J. Heterocycl. Chem.* **2006** (in press).
24. Fujita, F.; Ban, T. *J. Med. Chem.* **1971**, *14*, 148.
25. For a review, see Kubinyi, H. *Quant. Struct.-Act. Relat.* **1988**, *7*, 121.
26. Kubinyi, H. In *Encyclopedia of Computational Chemistry*; Wiley: New York, 1998 http://www.wiley.com/legacy/wileychi/ecc/samples/sample05 .
27. Derome, A. *Modern NMR Techniques for Chemistry Research*; Pergamon Press: Oxford, 1987, pp. 280.
28. Strekowski, L.; Tanious, F. A.; Chandrasekaran, S.; Watson, R. A.; Wilson, W. D. *Tetrahedron Lett.* **1996**, *27*, 6045, and references cited therein.